Int. J. Electrochem. Sci., 12 **(2017)** 8991 – 9006, doi: 10.20964/2017.10.74

International Journal of ELECTROCHEMICAL SCIENCE
www.electrochemsci.org

Corrosion Behavior of 316L Stainless Steel Coated by Chitosan/Gold/Nickel Nanoparticles in Mixed Acid Mixture Containing Inorganic Anions

Reham H. Tammam[*], *Amany M. Fekry*

Chemistry Department, Faculty of Science, Cairo University, Giza-12613, Egypt.
[*]E-mail: reham_tammam@cu.edu.eg

Received: 3 July 2017 / *Accepted:* 12 August 2017 / *Published:* 12 September 2017

The electrochemical behavior of 316L stainless steel alloy was performed by open circuit potential, electrochemical impedance spectroscopy, potentiodynamic polarization measurements and surface examination using scanning electron microscope technique in phosphoric and sulphuric acid solution mixtures with different percentages. The effects of inorganic additives (fluoride and iodide) on the corrosion of the tested alloy in mixed acidic mixture were also done. It was found that the corrosion rate decreases in the acidic mixture solution containing iodide than fluoride ion. However, electrodeposition of chitosan/Gold nanoparticles (AuNPs)/nickel nanoparticles (NiNPs) protects well the alloy surface in the most corroded solution of 0.005 M NaF. The efficiency increases according to the following order: coating $>I^-$ $>F^-$ > blank mixed acidic mixture. EIS results are in decent arrangement with polarization and open circuit potential results. All results are confirmed with surface examination.

Keywords: 316L stainless steel; coating; EIS, SEM and nanoparticles.

1. INTRODUCTION

Stainless steel alloys are well applied as corrosion resistant alloys. Phosphoric acid (P) is not very destructive elative to nitric or sulphuric acids(S)[1]. The presence of impurities for example fluorides, chlorides and sulphides cause severe corrosion in acidic solutions [1-3]. Materials choice is so important industrially. Stainless steel alloys have good chemical and mechanical properties [4], so, they are a good decision to be applied in phosphoric acid medium. A highly alloyed stainless steel (316L) offers the most resistance to corrosion in numerous standard services. It is well-known in practical application that 316L SS can be electrochemically polished in concentrated phosphoric-sulfuric mixed acids at higher temperatures larger than 65^{o}C [5]. The volume ratio of mixed acid used

for polishing stainless steel is set between 1:1 and 3:1 [6,7]. However, rare literatures have been accounted with respect to the effects of volume-ratio of the two mixed acids.

In this work a study of the behavior of 316L SS is performed in two inorganic acids (sulphuric and phosphoric acids)at different concentrations percentages both of which are important in the chemical manufacturing [8,9]. The effect of added ions such as fluoride and iodide were also established. The above issues are addressed in this examination.

To expand the stability of 316L stainless steel, a coating of chitosan, gold and nickel nanoparticles was added on alloy surface. Chitosan is an alkaline-deacetylated chitin resulting from skeletons of insects and shells of crustaceans. It is recommended owing to its excellent nontoxicity and adsorption properties [10]. Gold nanoparticles (GN) have good biocompatibility nanomaterials with high conductivity. Nickel is employed for corrosion inhibition with a well corrosion resistance in several corrosive media. Nickel content not only improves the physical and mechanical properties of stainless steel but also it enhances the corrosion inhibition behavior [11, 12].

Different techniques were utilized, for example, open circuit measurements (OCP), electrochemical impedance spectroscopy (EIS), potentiodynamic polarization and scanning electron microscopy (SEM).

2. EXPERIMENTAL

2.1. Materials preparation

Table 1. Chemical composition of the SS 316L (wt.%).

Composition Elements/wt%									
%Cr	**%Ni**	**%Mo**	**%Mn**	**%Cu**	**%N**	**%P**	**%C**	**%S**	**% Fe**
16.71	10.28	2.07	1.66	0.12	0.067	0.02	0.016	0.00006	balance

The tested 316L stainless steel rod has 0.2 cm^2 cross-sectional area and its composition is demonstrated in Table 1.

All the reagents used are of analytical grade acquired from Merck Products. Chemically ultra-pure 98% sulfuric acid (S) and 85% phosphoric acid (P) stock solutions are used for preparation of solutions (2M) by the appropriate dilution with doubly distilled water. Solutions of the inorganic acids were prepared using concentrations by volume percentage.

The surface of the electrode was mechanically polished to obtain smooth surface by emery papers with 400 up to 1000 grit, degreased in acetone, washed with ethanol and then dried in air.

Chitosan (CS) coating is performed by putting 0.1 g of CS in 100 ml 1% acetic acid solution and stirred for 5 hours. After that it added on the electrode surface and left to dry for 24 h and then immersed in 6 mM hydrogen-tetrachloroaurate $HAuCl_4$ solution containing 0.1 M KNO_3. After that -0.4 V vs. SCE is applied for 600s [13] to form gold nanoparticles. At the end electrodeposition of nickel nanoparticles (NiPs) on 316L stainless steel coated with CS/gold nanoparticles was achieved in one step. The potentiostatic deposition of metallic nickel on the working electrode (i.e., 316L stainless

steel) from an aqueous solution of 0.1 M acetate buffer solution (ABS, pH = 4.0) containing 1 mM $Ni(NO_3)_2 \cdot 6H_2O$ by applying a constant potential electrolysis at -1 V for 10 min time duration.

2.2. Electrochemical techniques

The cell used is three-electrode containing a large platinum sheet as a counter electrode (CE), saturated calomel (SCE) as a reference electrode (RE) and 316L stainless steel alloy as a working electrode (WE).

The electrochemical experiments carried out inside an air thermostat at 25^{o}C. Measurements were conducted in unstirred naturally aerated 2M sulfuric acid solutions in the presence of 2M phosphoric acid. Electrochemical impedance spectroscopy (EIS) technique was carried out using the electrochemical instrument (IM6 Zahner electric, Meβtechink, Germany). The amplitude used is 10 mV around the open circuit potential (E_{OCP}) and the scan frequency ranged from 0.1 Hz to 100 kHz.

Potentiodynamic polarization curves were scanned from -400 mV to +200 mVvs. SCE at a scan rate of 1 mV s^{-1}. Before each potentiodynamic polarization measurement, the system was left to stabilize for 2 h, with E_{OCP} being simultaneously measured. Duplicate tests for EIS and potentiodynamic polarization curves were carried out for all studied solution. The SEM micrographs were collected using a JEOL JXA-840A electron probe microanalyzer.

3. RESULTS AND DISCUSSION

3.1. Open circuit potentials results

Fig. 1 presents OCP measurements for 316L SS in (P) containing different concentration percentage of (S). At all the studied solutions the potential shifted positively suggesting a promising spontaneous film formation onto the surface, which reduces the alloy corrosion. Steady state potential(E_{st}) has the most positive value in 2M (P)(~200mV), whilst E_{st} has the most negative value in 2M (S) (~-20mV). From these results, in phosphoric acid the corrosion rates are found to be lower than those in sulphuric acid [14].

Generally, E_{st}, shifts negatively as S concentration increases, due to the damage of the oxide film and its continuous dissolution. Also, the potentials increase rapidly through the first 20 min and afterward shift gradually in the more positive direction. This action is due to the formation and growth of the oxide film on the surface of 316L SS.

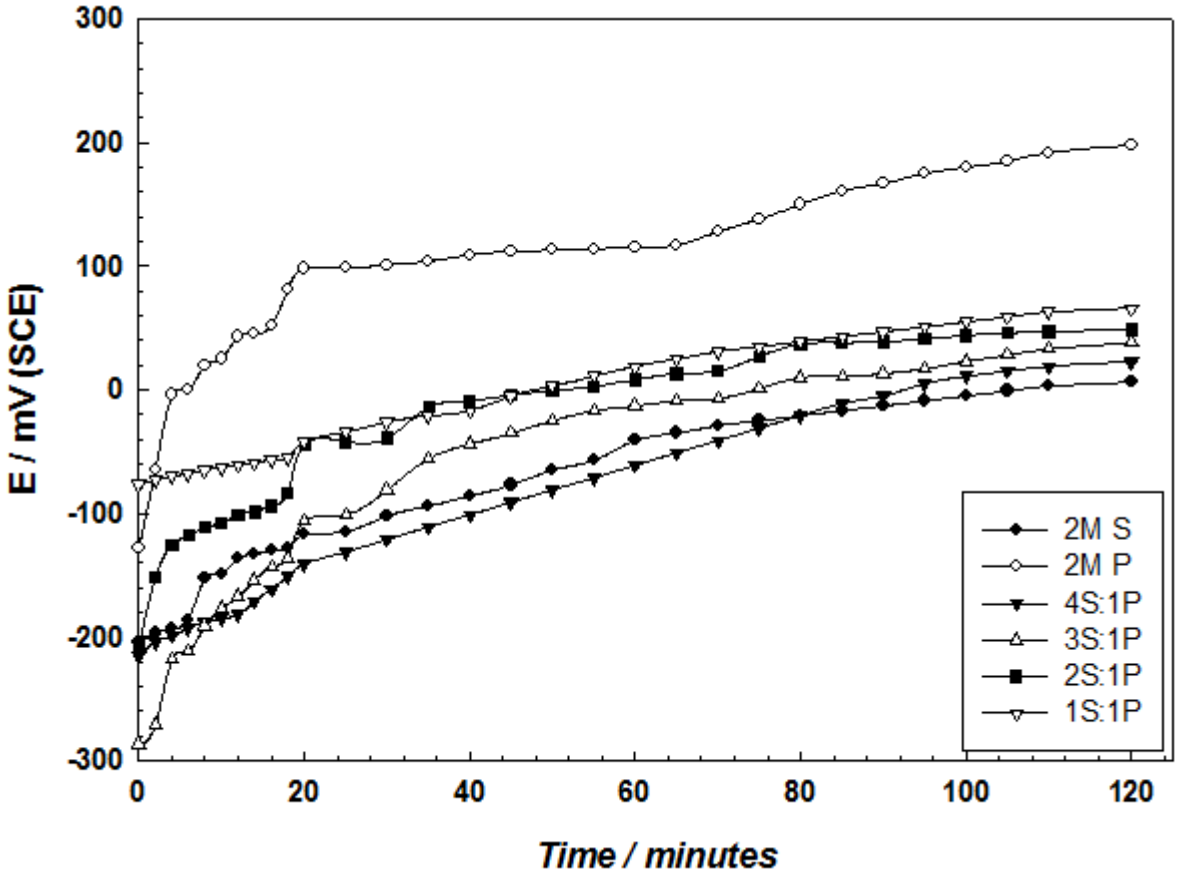

Figure 1. Variation of OCP for 316L SS alloy immersed in mixed H_3PO_4 and/or H_2SO_4 of different concentrations with immersion time. (○) 2M P, (v)1S:1P ,(■) 2S:1P , (Δ)3S:1P,(▼) 4S:1P ,(●) 2M S.

3.2. Impedance results

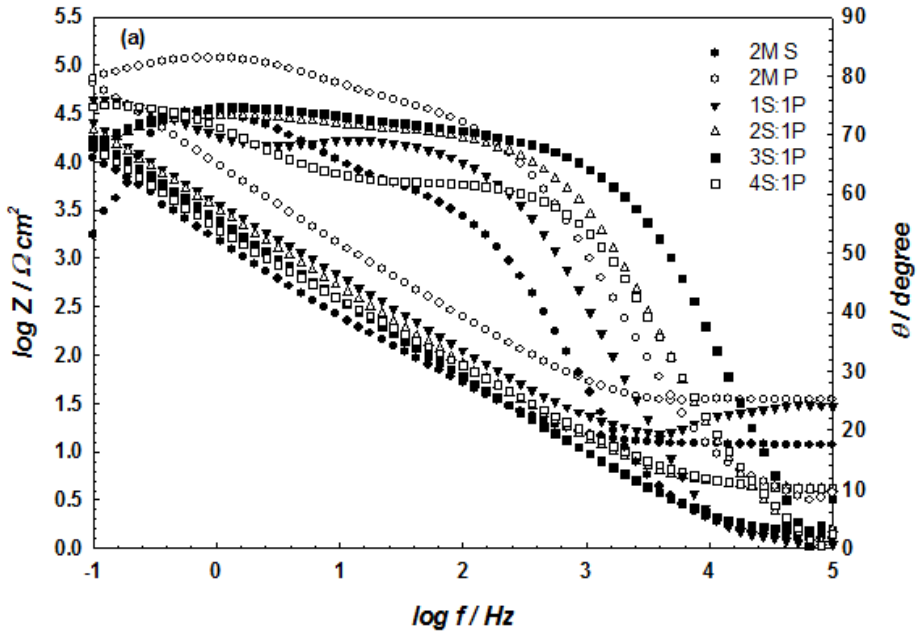

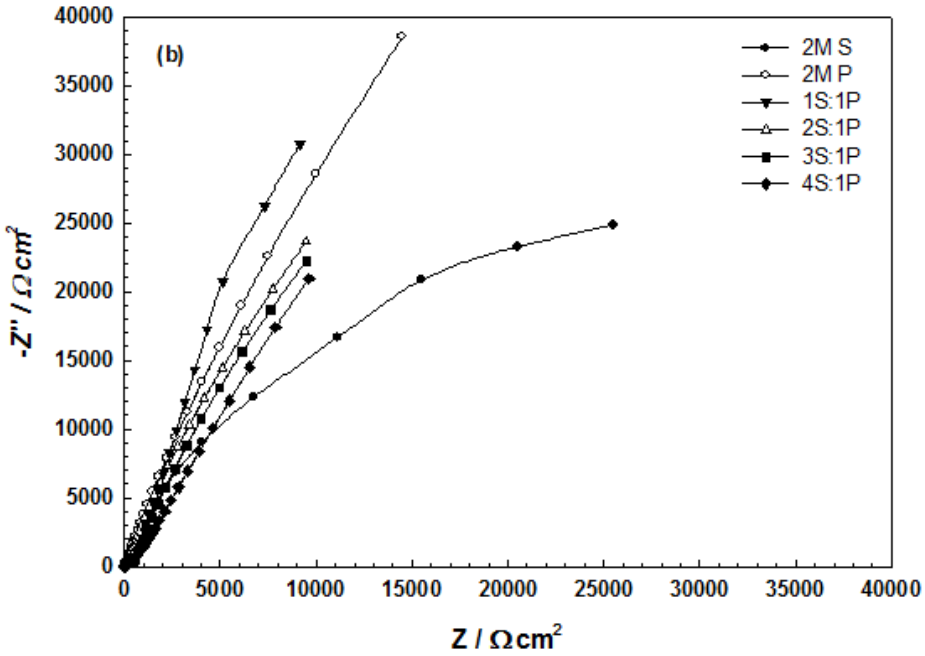

Figure 2. (a) Bode and (b) Nyquist plots of 316L SS alloy after immersion for 2h in mixed H_3PO_4 and/or H_2SO_4 of different concentrations.

EIS is an important technique to examine the corrosion behavior using corrosion inhibitors and/or polymer coatings [15–19]. Fig. 2 (a and b) shows the Bode and Nyquist plots for 316L SS in (P) at different (S) concentration percentage after immersion for 2h,respectively.Bode plots show a broad curves with a maximum phase angle near to 85^o. This indicates a passive behavior especially at 2M (P) compared to 2M (S). This behavior suggests that a protective layer against ion diffusion is formed in (P) [20]. The Nyquist plots also show the same behavior as that obtained from Bode plots. Thus, the impedance data are in a good agreement with the experimental OCP results (Fig. 1).

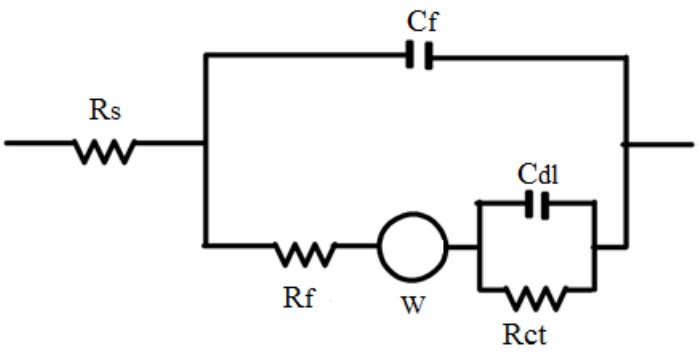

Figure 3. Equivalent circuit used in the simulation of the impedance data. R_s is the solution resistance, C_{dl} is the double layer capacitance; R_{ct} is the charge transfer resistance, C_f is the passive film capacitance, R_f is the passive film resistance and W is the diffusion "Warburg" impedance.

The impedance data were fitted by the equivalent circuit shown in Figure 3. The elements C_{dl} and C_f were treated as non-ideal capacitors for the double layer and the formed film, respectively and

estimated as constant phase elements (CPEs) [21]. CPE is characterized by the capacitance part in Farads and a dimensionless exponent part between 0 and 1. CPE is used instead of ideal capacitance to account for the surface heterogeneity. R_{ct} referred to a charge transfer resistance, R_f referred to film resistance and W referred to Warburg impedance owing to diffusion process [22]. Table 2 gives the fitted impedance data carried out in H_3PO_4 at different H_2SO_4 concentration percentage after immersion for 2h.

Table 2. Equivalent circuit parameters for 316L SS alloy immersed in mixed H_3PO_4 (P)and/or H_2SO_4(S)of different concentration percentageafter 2 h.

Acid Ratio	R_f ($M\Omega\ cm^2$)	R_{Ct} ($K\Omega\ cm^2$)	C_f ($\mu F\ cm^{-2}$)	C_{dl} ($\mu F\ cm^{-2}$)	Z_w ($k\Omega\ s^{-1}$)	R_s ($\Omega\ cm^2$)
2M S	5.3	12.6	38.4	76.3	12.2	15.9
1S:1P	16	25.2	18.5	64.3	53.1	21.6
2S:1P	19	50.1	21.7	60.5	47.3	14
3S:1P	21	65.2	26.1	56.8	40.9	18
4S:1P	25	68.1	30.6	53.2	31.8	10
2M P	61	119	12.5	47.5	61.6	21

From which, R_f value in presence of 2M (S) was 5.3 $M\Omega\ cm^2$, however, as the concentration of P increase, the R_f values increases reaching to 61 $M\Omega\ cm^2$; this was attributed to that, as mentioned in OCP, the corrosion rates in phosphoric acid are lower than those calculated in sulphuric acid solution [14]. Also, C_{dl} values decrease from 76.3$\mu F\ cm^{-2}$ (in 2M S) to 47.5 $\mu F\ cm^{-2}$(in 2M P) which indicates an increase in film relative thickness which is equal to $1/C_{dl}$.

Table 3. Equivalent circuit parameters for 316L SS alloy immersed in mixed H_2SO_4 (S) and/or H_3PO_4 (P) of different concentration percentage after 2 h.

Acid Ratio	R_f ($M\Omega\ cm^2$)	R_{Ct} ($K\Omega\ cm^2$)	C_f ($\mu F\ cm^{-2}$)	C_{dl} ($\mu F\ cm^{-2}$)	Z_w ($k\Omega\ s^{-1}$)	Rs ($\Omega\ cm^2$)
2M S	5.3	12.6	38.4	76.3	12.2	15.9
1S:1P	16	25.2	18.5	64.3	53.1	21.6
1S:2P	39	89	16.5	51.7	57.2	15.6
1S:3P	45	96	15.3	50.1	59.5	13.7
1S:4P	53	107	14.0	49.7	60.3	18.1
2M P	61	119	12.5	47.5	61.6	21

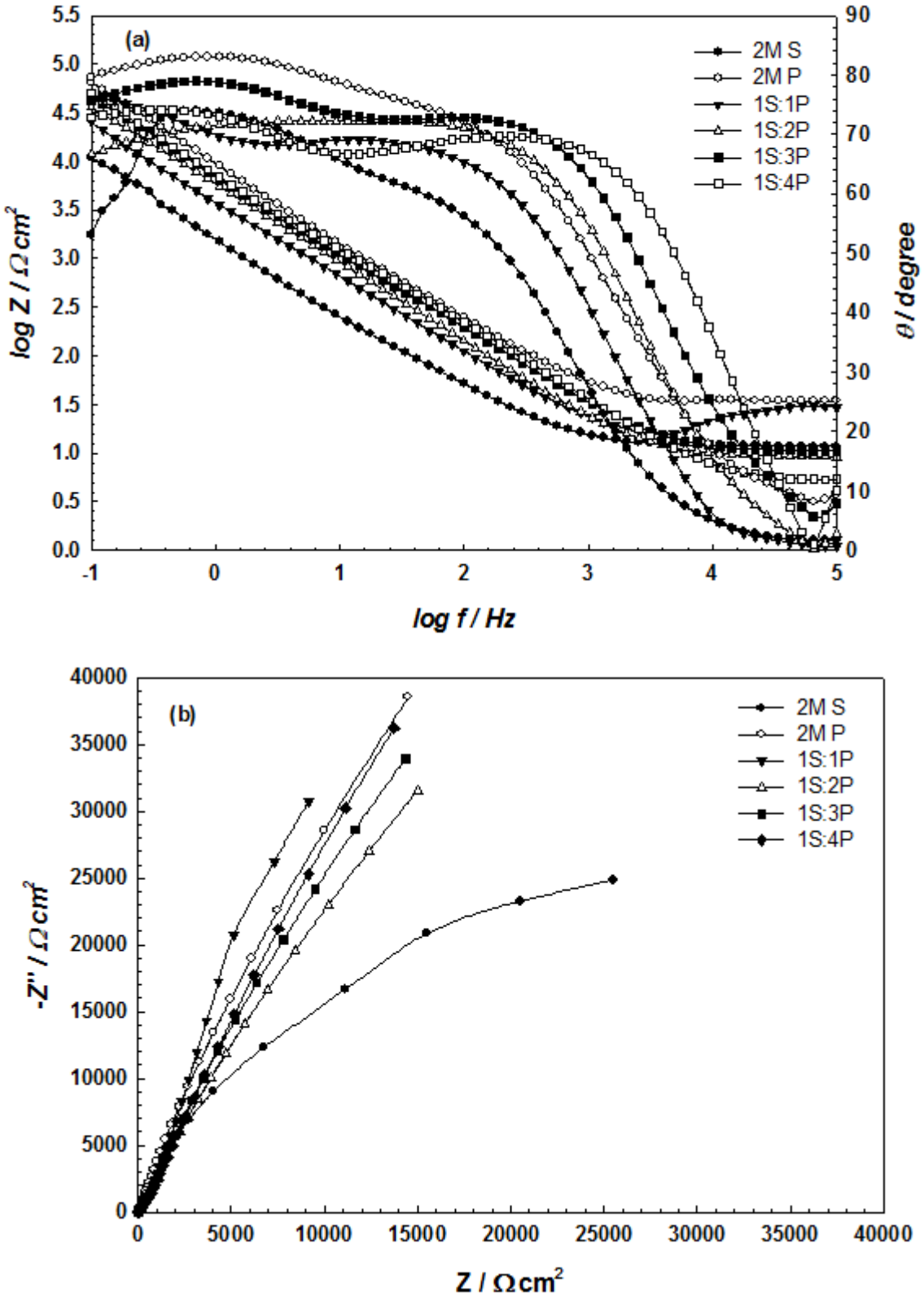

Figure 4. (a) Bode plots (b) Nyquist plots of 316L SS alloy after immersion for 2h in mixed H_2SO_4 and/or H_3PO_4 of different concentrations.

Bode and Nyquist representations of the impedance values of the 316L SS in S at different P concentration percentage after 2h are shown in Figure 4a and b. It is noticed that as the concentration of P increases, the impedance values increase. The Bode plots have the same shape like that in Fig. 2a

with the same mechanism. The Nyquist plots 2b and 4b show linear-like rather than arc-like behavior over the frequency range examined, which suggests that corrosion does not appreciably occur [23]. The data was also fitted with the same model shown in Fig. 3 and fitting parameters are given in Table 3.

Bode plots of 316L SS in both ions (fluoride or iodide) solution are displayed in Fig.5 and 6, respectively. By studying the effect of adding either fluoride or iodide to 1S:1P v/v mixed acid solution, it was found that the impedance value increases with increasing the concentration of both ions (fluoride or iodide), as shown in Fig. 5 and 6, respectively. At low frequencies (<1Hz), total impedances of different fluoride or iodide concentrations are higher than the blank solution 1S:1P v/v mixed acid.

Table 4. Equivalent circuit parameters for 316L SS alloy immersed in 1S:1P solution with different concentrations of NaF and NaI after 2 h.

Salt	C_{anion} (M)	R_f ($M\Omega\ cm^2$)	R_{Ct} ($K\Omega\ cm^2$)	C_f ($\mu F\ cm^{-2}$)	C_{dl} ($\mu F\ cm^{-2}$)	Z_w ($k\Omega\ s^{-1}$)	R_s ($\Omega\ cm^2$)
NaF	0	16	25.2	18.5	64.3	53.1	21.6
	0.005	31.6	70.7	17.9	51.0	60.5	31.8
	0.01	33.8	73.5	17.5	50.7	63.4	32.4
	0.025	37.1	75.4	17.3	50.4	69.1	30.5
	0.05	40.0	78.9	17.0	49.7	75.3	29.3
NaI	0.005	47.8	100.3	15.3	43.1	57.4	32.5
	0.01	56.2	132	11.4	35.7	60.5	31.2
	0.025	87.1	145	10.3	30.1	67.3	30.9
	0.05	125.8	176	9.5	23.7	70.5	29.4

Table 5. Equivalent circuit parameters for coated and uncoated 316L SS alloy immersed in 1S:1P solution containing 0.005 M NaF after 2 h.

composition	R_f ($M\Omega\ cm^2$)	R_{Ct} ($K\Omega\ cm^2$)	C_f ($\mu F\ cm^{-2}$)	C_{dl} ($\mu F\ cm^{-2}$)	Z_w ($k\Omega\ s^{-1}$)	R_s ($\Omega\ cm^2$)
0.005 M NaF	31.6	70.7	17.9	51.0	60.5	31.8
CS	158.4	112.5	10.5	24.1	-	30.8
CS/Au	251.1	150.6	6.4	19.4	-	30.4
CS/Au/Ni	316.2	209.4	3.1	11.7	-	30.7

Analyzing the impedance parameters shown in Table 4, it can be seen that in iodate solution at all concentrations, both R_f and R_{ct} indicate a better corrosion resistance compared to that of fluoride solution. These impedance parameters give indications that independently of the nature of the electrolyte (iodate or flouride) provide a better corrosion resistance than the blank 1S:1P v/v mixed solution. Later studies also proved that introduction of an oxidising agent like KIO_3 into a corrosive acidic medium can lead to self-passivation of steel [24].

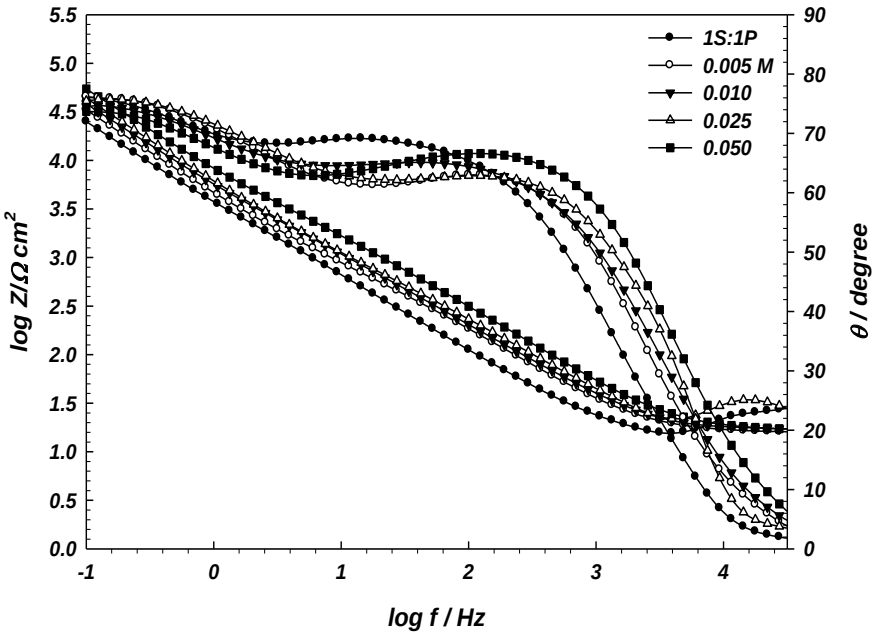

Figure 5. Bode plots of 316L SS alloy immersed for 2 h in 1S:1P v/v mixed acid solution with NaF of various concentrations: (●) 0 M, (○) 0.005 M, (▼) 0.01 M, (Δ) 0.025 M and(■) 0.05M.

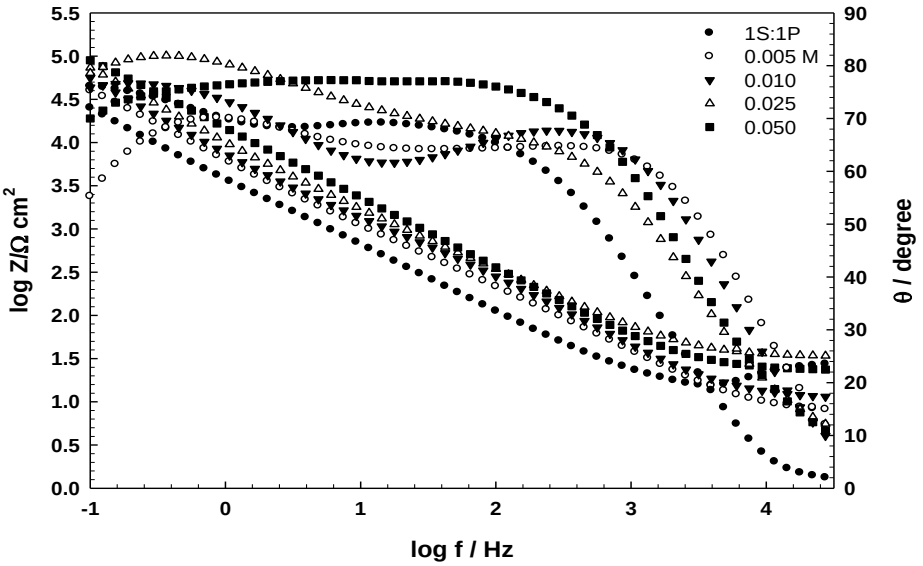

Figure 6. Bode plots of 316L SS alloy immersed for 2 h in 1S:1P v/v mixed acid solution with NaI of various concentrations: (●) 0 M, (○) 0.005 M, (▼) 0.01 M, (Δ) 0.025 M and(■) 0.05M.

Studies were also reported with iodate as an effective corrosion inhibitor for copper in acidic solutions as it acts as an oxidizer at low concentrations and at higher concentrations it acts as a passivator for the dissolution of copper, with good adsorption of these iodate ions on copper surface,

forming $Cu(IO_3)_2$ [25]. This work ensures this phenomenon that iodate ions are better than flouride ions.

From Figs. 5 and 6, it were understood that the strength of the passive film increases with the increase in the concentration of the original passivator solution [26, 27].

Fig.7 represents Bode plots of coated 316L SS exposed after 2 h immersion in 1S:1P v/v mixed acid solution containing 0.005 M NaF (most corrosive medium). It was observed that chitosan coatings reduced drastically the corrosion rate then adding gold nanoparticles lowers more the corrosion rate of 316L SS and then adding Ni nanoparticles decreases it well. At first adding chitosan only with high adsorption properties on 316L stainless steel alloy that decreases its corrosion rate in this corrosive medium [10].

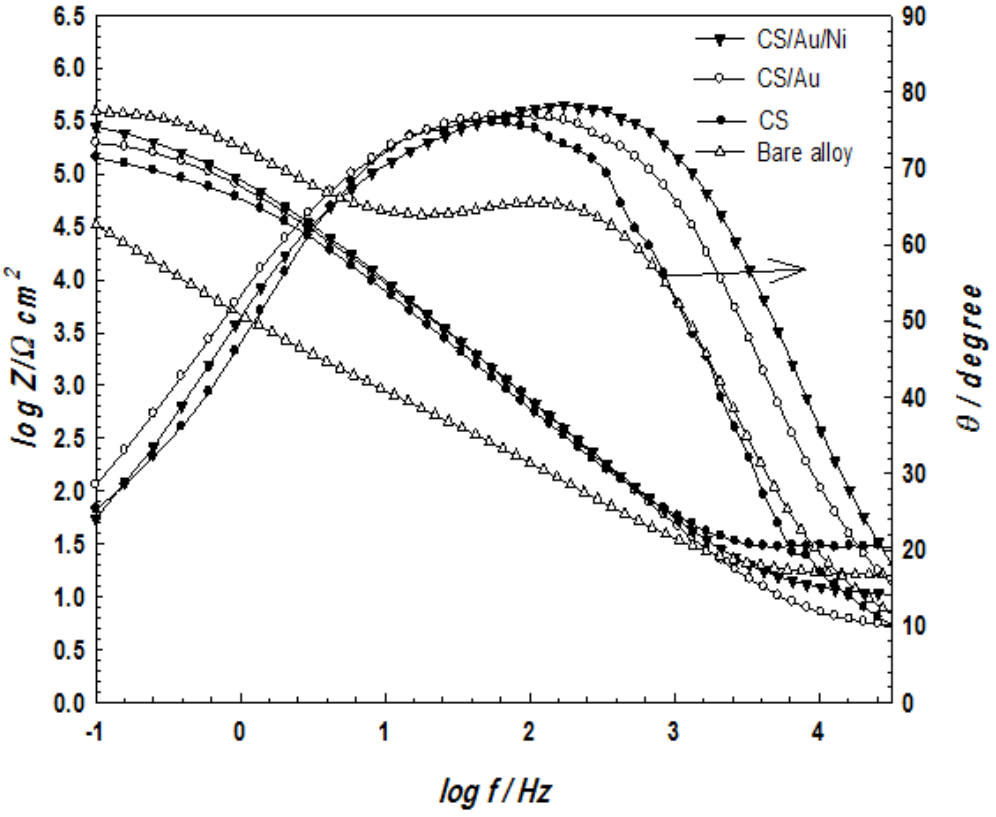

Figure 7. Bode plots of coated and uncoated316L SS alloy after 2 h immersion in 1S:1P v/v mixed acid solution containing 0.005 M NaF.(Δ)Bare alloy, (●)CS, (○)CS/Au, (▼)CS/Au/Ni.

Then adding gold nanoparticles spreading electrochemically well on the surface increasing its stability and then adding Ni nanoparticles gives the highest corrosion resistance. This is known well due to nickel ions lowers corrosion rate [28].

3.3. Polarization results

Potentiodynamic polarization curves of the 316L SS in 1S:1P v/v mixed acids containing 0.005M NaF, 0.005M NaI and/or CS/Au/Ni nanocomposite coated alloy in 1S:1P v/v mixed mixture containing 0.005 M NaF (most corrosive medium), were shown in Fig.8.

The presence of the CS/Au/Ni nanocomposite and/or inorganic ions (F^- and I^-) cause the decrease in the corrosion rate as can be seen from the shift of the cathodic polarization curves to more negative potentials and the anodic ones to more positive values. This performance could be attributed to the adsorption of fluoride and iodide and /or CS/Au/Ni nanocomposite or their reduction products on the metal or metal oxide surface [29]. The existence of these anions causes the shift of E_{corr} to less negative values with an obvious decrease in the corrosion current density, i_{corr}. On coatings with CS/Gold/NiPs, i_{corr} is the smallest value compared to the other anions with broad current plateau is observed in the anodic branch, due to a passivation process [30, 31]. The current values stay constant and are followed by an increase in the anodic polarization. Compared with the blank 1S:1P solution, there is a considerable decrease in the i_{corr} values.

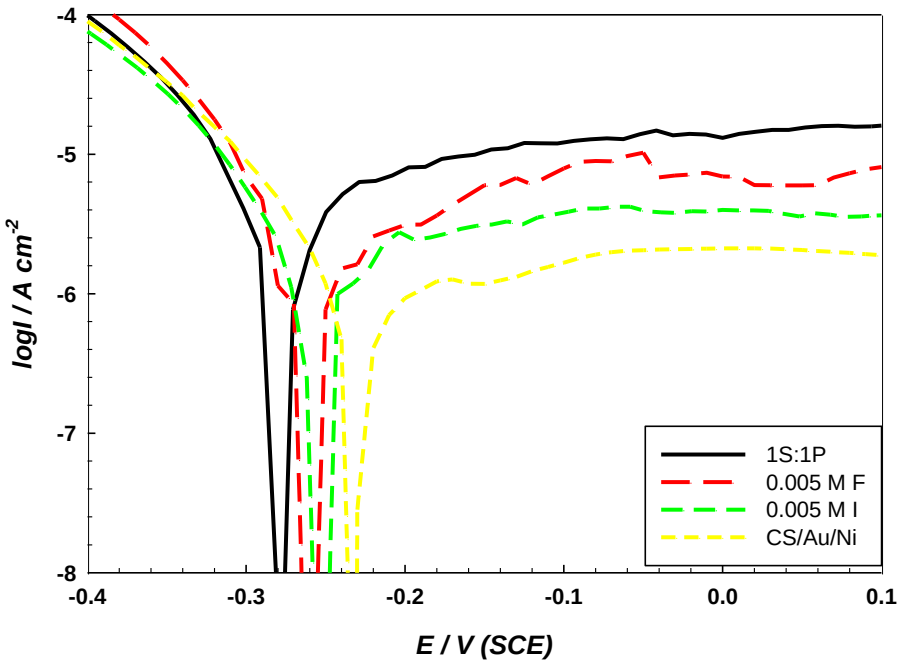

Figure 8. Potentiodynamic polarization curves for uncoated 316L SS alloy after 2 h immersion in 1S:1P v/v mixed acid solution containing: 0.005M NaF, 0.005M NaI and/or CS/Au/Ni coated 316L SS alloy in 1S:1P v/v mixed acid solution containing 0.005M NaF.

The i_{corr} was obtained from Tafel plots using both the cathodic and anodic branches of the polarization curves. As depicted in Fig. 8 and Table 6, i_{corr} of about 3.16 (±0.25) μA cm^{-2} associated with a corrosion potential of about -280 mV (SCE) is observed for the blank 1S:1P solution. For fluoride ions, i_{corr} and E_{corr} values of about 1.99(±0.24)μA cm^{-2}; -260mV (SCE) are observed and for iodide ions, i_{corr} and E_{corr} values are 0.98(±0.23)μA cm^{-2}; -250 mV (SCE). With respect to CS/Au/Ni

nanocomposite, the i_{corr} and E_{corr} values of about 0.63 (±0.25)μA cm^{-2}; -220 mV (SCE) are evaluated. E_{corr} increase in the following order: blank (1:1) < F^- < I^- < CS/Au/Ni nanocomposite, which is the same order reported previously for these additives to act as passivators for the corrosion of 316L SS in 1S:1P solution using EIS technique.

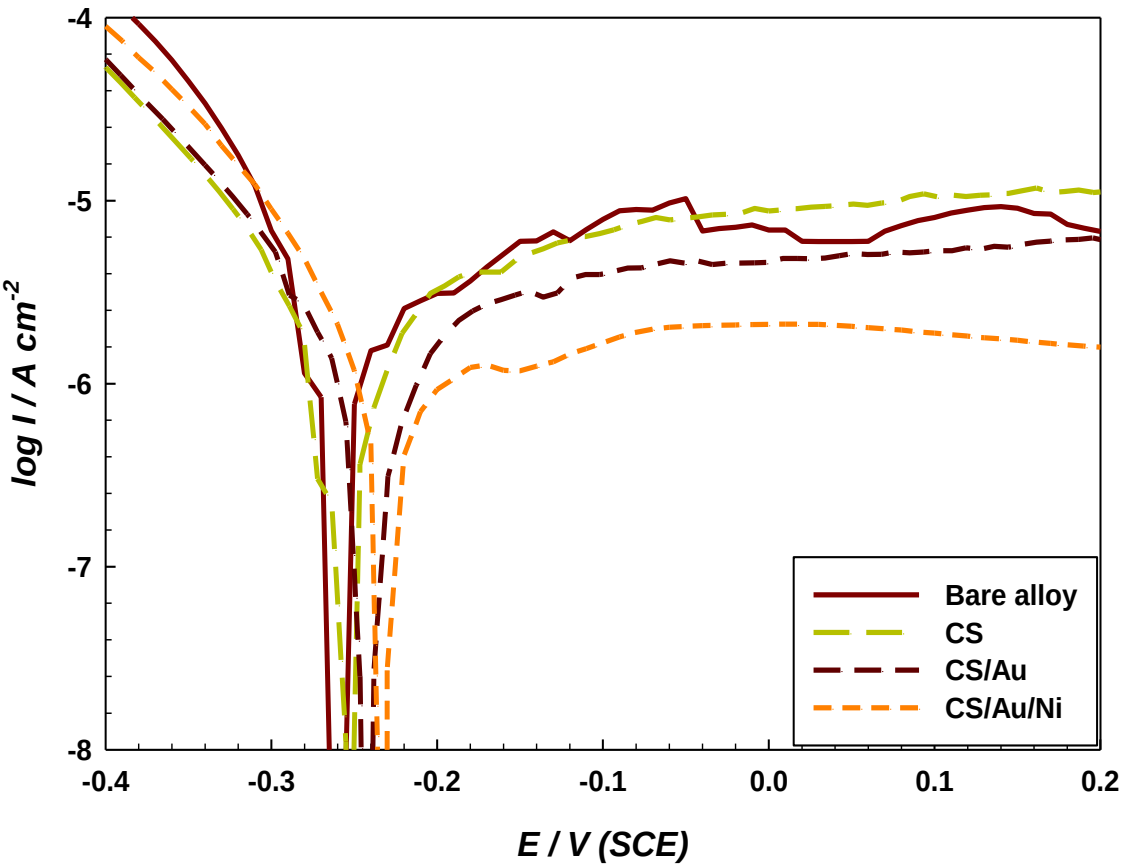

Figure 9. Potentiodynamic polarization curves for coated and uncoated 316L SS alloy after 2 h immersion in 1S:1P v/v mixed acid solution containing 0.005 M NaF.

The curves of Fig. 9 represent the anodic and cathodic scans, E-log i, of 316L SS in 1S:1P solution at different coats on 316L stainless steel alloy. As can be seen; a shift of E_{corr} values toward the nobler potential side with a decrease in i_{corr} values in the following order for coats (CS < CS/AuNPs < CS/Au/Ni nanocomposite) considering that 316L SS has higher corrosion resistance in a 1S:1P solution containing 0.005 M NaF.

After CS/Au/Ni nanocomposite coating for test alloy, it showed a higher E_{corr} value of -220mV(SCE) with a lower i_{corr} value 0.63(±0.25) μA cm^{-2} as compared to -280 mV (SCE) and 3.16 (±0.25)μA cm^{-2} is observed for the blank 1S:1P (as shown in Table 7).

The addition of Ni to CS/Au nanocomposite leads to a decrease in corrosion current density (i_{corr}) and an increase in corrosion resistance (R_{corr})[32].

Table 6. Electrochemical corrosion parameters from Tafel results for uncoated 316L SS alloy in 1S:1P v/v mixed acid solution containing: 0.005M NaF, 0.005M NaI and/or CS/Au/Ni coated 316L SS alloy in 1S:1P v/v mixed acid solution containing 0.005M NaF after 2 h immersion.

	$-\beta_c$/ mV dec^{-1}	β_a/ mV dec^{-1}	I_{corr}/ µA cm^{-2}	E_{corr}/ mV
Blank(1S:1P)	159	78	3.16	-280
0.005M NaF	172	85	1.99	-260
0.005M NaI	195	86	0.98	-250

Table 7. Potentiodynamic polarization parameters for coated and uncoated 316L SS alloy in 1S:1P v/v mixed acid solution containing 0.005 M NaF after 2 h immersion

	$-\beta_c$/ mV dec^{-1}	β_a/ mV dec^{-1}	I_{corr}/ µA cm^{-2}	E_{corr}/ mV
Bare alloy	159	78	3.16	-280
CS	177	86	2.76	-284
CS/Au	161	86	2.18	-273
CS/Au/Ni	187	84	0.63	-220

3.4. SEM measurements

(a)

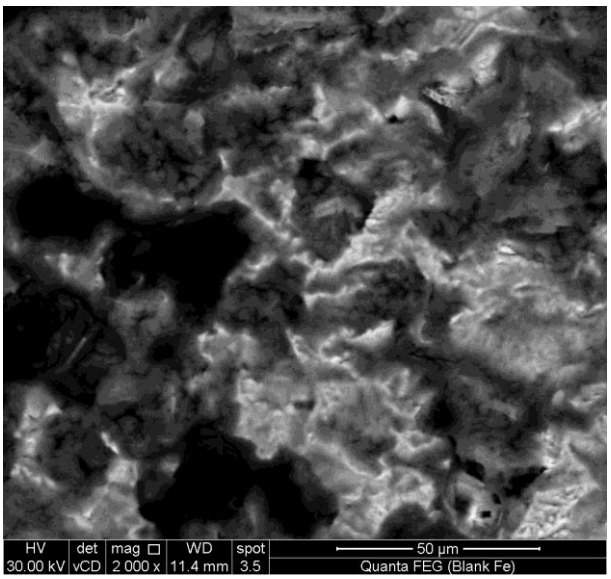

(b)

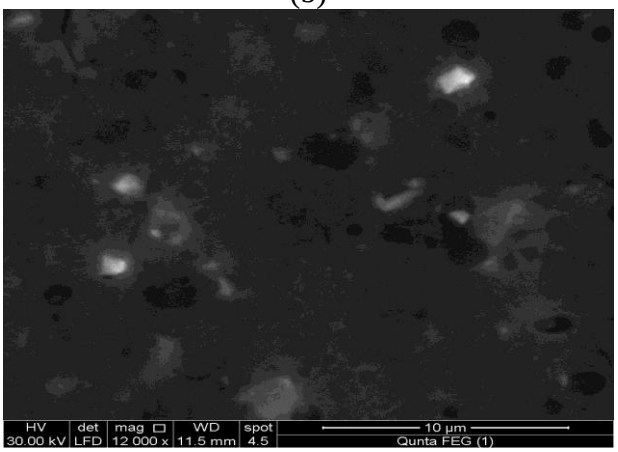

(c)

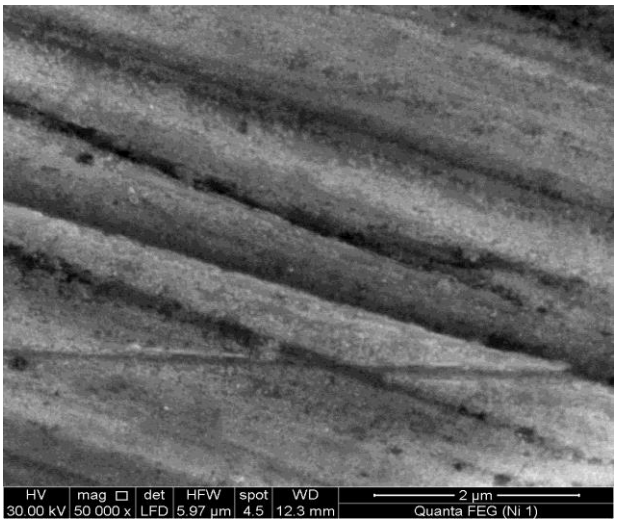

Figure 10. SEM-micrograph presenting the surface morphology of 316L SS alloy after 2h immersion in a) 1S:1P v/v mixed acid containing b) 0.005 M NaF and c) CS/Au/Ni coated alloy in 0.005 M NaF.

The SEM analysis of the morphology for the corroded surfaces after the immersion tests permitted the identification of more details. Fig.10 shows the SEM photos of 316L SS surface in 1S:1P v/v mixed acid. Fig. 10a shows that after immersion of 316L SS surface in unpassivated 1S:1P show an aggressive attack of the corroding acidic medium on the steel surface and the surface layer is rather rough. In contrast, in the presence of 0.05 M NaF, 0.05 M NaI and Cs/Gold/NiPs (10 min), Fig. 10b-c shows that the corrosion is drastically passivated. There is an adsorbed film on 316L SS surface at the studied three ions (Fig. 10b-c) which does not exist in corresponding

Fig.10a. In accordance, it could be concluded that the adsorption film can efficiently passivated the corrosion of 316L SS. Also, CS/Au/Ni nanocomposite decreases the corrosion of 316L SS perfectly than NaI and NaF solutions alone. The corrosion was more severe on the 316L SS when compared with the inorganic additives.

4. CONCLUSIONS

The corrosion behavior of uncoated or coated 316L stainless steel in phosphoric and sulphuric acid mixture solution; in the absence and presence of iodide, fluoride was investigated using different electrochemical techniques and surface analysis. From the results obtained, the following conclusions could be drawn:

(i) The rate of oxide film destruction in presence of inorganic additives (fluoride, iodide) decreases with increasing their concentration and depends on anion type.

(i) The presence of fluoride, iodide enhances the passivation action of the alloy. The passivation efficiency decreases well on coating 316L stainless steel alloy with CS/Au/Ni nanocomposite.

(ii) SEM analysis on the surface of corroded samples confirmed that the introduction of CS/Au/Ni nanocomposite into 1sulfuric:1phosphoric mixed acid solution containing 0.005 M NaF effectively protects 316L stainless steel from corrosion.

References

1. R. Tammam, A. Fekry and M. Saleh, *Int. J. Electrochem. Sci.*, 11 (2016) 1310.
2. S. El Hajjaji, L. Aries, J. Audouard and F. Dabosi, *Corros. Sci*., 37(1995) 927.
3. H. Iken, R. Basseguy, A. Guenbour and A. Bachir, *Electrochim. Acta*, 52 (2007) 2580.
4. A. Guenbour, M. Hajji, E. Jallouli and A. Bachir, *Appl Surf. Sci*., 253(2006) 2362.
5. D. Landolt, *Electrochim. Acta*, 32 (1987) 1.
6. S. Chen, H. Huang and Y. Pan, *Corros. Sci.*, 48 (1992) 594.
7. A. Fekry, R. El-Kamel and A. Ghoneim, *J. Materials Chemistry B*, 4 (2016) 4542.
8. E. Otero, A. Pardo, E. Sáenz, M. Utrilla and P. Hierro, *Corros. Sci*., 38(1996)1485.
9. E. Otero, A. Pardo, M. Utrilla, F. Pérez and C. Merino, *Corros. Sci.*, 39 (1997)453.
10. A. Fekry, *RSC Adv*., 6(2016)20276.
11. R. Revie, H. Uhlig , *Corrosion and Corrosion Control*, Wiley Interscience, New Jersey, 2008, pp.407–418.
12. A. Grayeli-Korpi and H. Savaloni, *Appl. Surf. Sci*., 258 (2012) 9982.
13. R. Farghali, A. Fekry, R. Ahmed and H. Elhakim, *Int. J. Biological Macromolecules,* 79 (2015)787.
14. E. Otero, A. Pardo, M. Utrilla, E. Enz and J. Alvarez, *Corros .Sci*., 39(1998)1421.
15. F. Mansfeld, S. Jeanjaquet and M. Kendig, *Corros. Sci*., 26 (1986)735.
16. W. Lorenz and F. Mansfeld, *Corros. Sci*, 21(1981)647.
17. G. Walter, *Corros. Sci.*, 26 (1986) 681.
18. F. Mansfeld, *Electrochim. Acta,* 35 (1990) 1533.
19. F. Mansfeld, H. Xiao, L. Han and C. Lee, *Progress in Organic Coatings,* 30(1997) 89.
20. S. Chen, G. Tu and C. Huang, *Surf.& Coat Tech*., 200 (2005)2065.
21. V. Lliev and D. Pavlov , *J. Electrochem. Soc.*, 129 (1982)458.
22. M. Huković and R. Babić and S. Brinić, *J Power Sources,* 157 (2006) 563.
23. S. Zhang and T. Jow, *J Power Sources*, 109(2002)458.
24. S. Shibli and V. Saji, *Corros. Sci*., 47 (2005) 2213.
25. Q. Luo, *Langmuir* ,16 (2000) 5154.
26. M. Kappes, M. Ortíz, M. Iannuzzi and R. Carranza, *Corros. Sci.*, 73(2017)31.
27. E. Abd El Aal, S. Abd El Wanees, A. Farouk and S. Abd El Haleem, *Corros. Sci*., 68(2013)14.

28. A. Fundo and L. Abrantes, *J. Electronal. Chem*., 600 (2007) 63.
29. S. Abd El Wanees and E. Abd El Aal, *Corros. Sci*., 52 (2010) 338.
30. S. Yalçınkaya and D. Çakmak , *J. Molecular Structure* ,1135 (2017) 32.
31. P. Lo, W. Tsai, J. Lee and M. Hung, *Surf. Coat. Technol*., 67(1994)27.
32. H. Sorkhabi and M. S'haghi, *Corros. Sci*., 77(2013)185.